Available online at www.sciencedirect.com
SCIENCE DIRECT®
Journal of Nuclear Materials 335 (2004) 115–120
journal of nuclear materials
www.elsevier.com/locate/jnucmat

Temperature dependence of liquid Sn sputtering by low-energy He^+ and D^+ bombardment

M.D. Coventry *, J.P. Allain [1], D.N. Ruzic

Plasma–Material Interaction Group, University of Illinois at Urbana-Champaign, 103 S. Goodwin Avenue, Urbana, IL 61801, USA

Received 22 March 2004; accepted 24 June 2004

Abstract

Absolute sputtering yields of liquid tin from 240 to 420 °C due to irradiation by low-energy helium and deuterium have been measured. For ion energies ranging from 300 to 1000 eV, temperature enhancement of liquid tin sputtering was noted. These measurements were obtained by IIAX (the Ion-surface InterAction eXperiment) using a velocity-filtered ion beam at 45° incidence to sputter material from a liquid tin target onto deposition monitors. Sputtering yields from 500 eV ion bombardment at 45° incidence increase from 0.1 ± 0.03 and 0.019 ± 0.008 Sn particles/ion at room temperature, for He^+ and D^+ ions respectively, to 0.30 ± 0.12 and 0.125 ± 0.05 Sn particles/ion for 380 °C. Temperature enhanced sputtering has been seen in other liquid metals (namely lithium, tin–lithium, and gallium) using both ion beam and plasma irradiation.

PACS: 52.40.H; 28.52.F; 79.20.R

1. Introduction

Liquid tin is one of several promising liquid metals under consideration for use as a divertor plasma-facing component (PFC) in future fusion machines with high power flux and high duty cycle [1]. Motivating factors for using a flowing liquid metal include rapid removal of heat and infinite component lifetime (no net erosion or damage of PFC). The principal advantage of using tin, in particular, is that it has the lowest vapor pressure among candidate liquid metals (Li, Ga, Sn–Li) [2] in the temperature range of 232–1000 °C. The low vapor pressure allows a wider temperature range of operation, resulting in greater flexibility in design and the potential for improved thermal efficiency for energy conversion. It has been estimated that the evaporation-limited upper operating temperature for tin could be as high as 1500 °C [1]. Tin's primary drawbacks are its high atomic number, minimizing the acceptable impurity level, and its smaller thermal conductivity in comparison to lithium [3]. However, it is also important to consider any enhancement of the sputtering yield with temperature to determine a realistic upper limit on operating temperature of the liquid as many liquid metals (and several solids) have shown temperature-enhanced sputtering properties [4–7].

Tin interacts weakly with hydrogen; thus, it is expected not to retain impinging tritium in a D–T reactor. Low retention of tritium helps reduce the tritium

* Corresponding author. Tel.: +1 217 333 6291; fax: +1 217 333 2906.
E-mail address: coventry@uiuc.edu (M.D. Coventry).
[1] Present Address: Argonne National Laboratory, Argonne, IL 60439.

0022-3115/$ - see front matter © 2004 Elsevier B.V. All rights reserved.
doi:10.1016/j.jnucmat.2004.06.009

inventory and simplifies the necessary handling precautions associated with removing tritium from the material. This will prove especially important for advanced, high-power machines that will be DT-fueled and contain a considerable amount of tritium. Another potential application of liquid tin under plasma bombardment is in extreme ultra-violet (EUV) light sources for photolithography [8], whose successful development would also require temperature-dependent information.

Any use of liquid metal subject to plasma bombardment requires an understanding of the possible temperature dependence on sputtering behavior. Liquid lithium, another candidate for both fusion and EUV applications, has been shown [4,5] to have a strong temperature-dependent sputtering yield under low-energy ion (including self [9,10]) bombardment. Results from studies using a 700 eV ion beam [4] and another using a plasma source with 75 eV ion energies [5] exhibited one to two orders of magnitude increase, respectively, in the absolute sputtering yield as the surface temperature was raised from 200 to 420 °C. Liquid gallium has also been shown to have appreciable temperature-dependent sputtering properties in the PISCES-B experiment [6] at a level below that of lithium. Gallium's sputtering yield by 100 eV deuterium ions increases by roughly a factor of two over the same temperature range. While PISCES-B greatly differs from IIAX, as it uses plasma to bombard the surface as opposed to a monoenergetic ion beam, the temperature-dependent sputtering yield for Li, Ga, Sn–Li, and Sn seems to be an intrinsic property of these, and other, materials.

2. Experiment

In the IIAX experiments, the physical sputtering yield of both solid and liquid tin was measured from a 4-mm diameter sample under D^+ and He^+ irradiation at incident energies of 300–1000 eV and sample temperatures ranging from room temperature up to 420 °C. A section of high-purity tin foil was installed within a stainless steel retention ring between a heated backing plate and a tantalum evaporative shield following being cleaned by ex situ mechanical scraping. Following evacuation of the chamber to a base pressure on the order of 10^{-7} Pa, the tin sample is heated past its melting point of 232 °C to a number of predetermined temperatures. The liquid tin surface is again scraped, this time in vacuo to remove any macroscopic contaminants on the surface, revealing a highly reflective surface. We have great confidence in the cleanliness of the surface of the liquid tin target for two reasons: the low base pressure and evidence noted by Bastasz et al. using low-energy ion scattering and direct-recoil spectroscopy (LEIS/DRS) [11,12] that liquid tin surfaces are relatively oxygen-free, at least up to 800 °C. They showed that even upon cooling and resolidification the surface was found to be effectively oxygen-free. This is an important issue with tin, in particular, as the sputtering yield of oxidized tin is roughly double that of the pure metal case [13], in contrast to most metals and their oxides.

The principal components of IIAX are a differentially pumped ion gun, a target chamber that reaches base pressures in the low 10^{-7} Pa regime, a target holder/heater assembly, and a dual crystal unit quartz crystal microbalance (DCU-QCM) mounted on an XYZΘ manipulator. Fig. 1 depicts the IIAX experimental target region. The Colutron ion source employed extracts ions from a DC discharge of the desired gas with the aid of a hot tungsten cathode (or thermionic emission from a solid source). An ion beam is extracted by a set of lenses, accelerated up to at least 700 eV, and then passes through a Wien filter to remove all but the desired ion species from the beam. The beam then passed through a series of ion beam optics for transport and focusing. As IIAX has a long working (source to target) distance, space–charge effects can dominate if the ions within the beam are allowed to interact with each other for an extended time. To reduce space–charge-induced beam divergence, the ion beam energy at or above 700 eV for a majority of the beam length. A decelerator in front of the target is used for beam energies less than 700 eV. The sample is irradiated by an ion flux on the order of 10^{17}–10^{18} $m^{-2}s^{-1}$ until a specified dose, typically around 10^{16} ions, is obtained at an incident angle set at 45° from the target surface normal for this study.

A deposition crystal collects a fraction of the eroded flux from the liquid tin sample. This crystal is one of two quartz crystal oscillators (QCO) that act as microbalances to determine the mass of material collected.

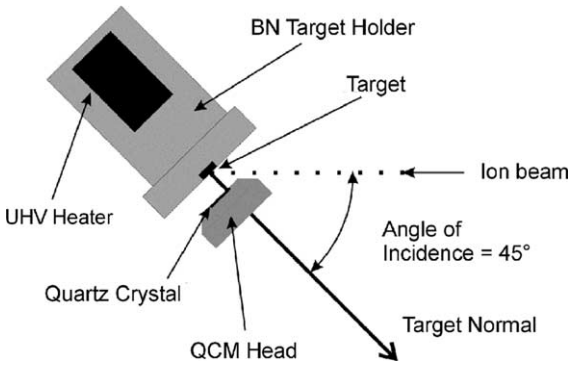

Fig. 1. A simplified schematic of the target/collector region in IIAX. This is a view looking down; the collector crystal is bombarded by about 13% of the material sputtered from the crystal due to geometric effects. The reference crystal is located almost 3 cm directly above the collector crystal and only sees 0.06% of the sputtered material; this is neglected do to a very low sticking coefficient determined by VFTRIM for the case of very oblique incidence.

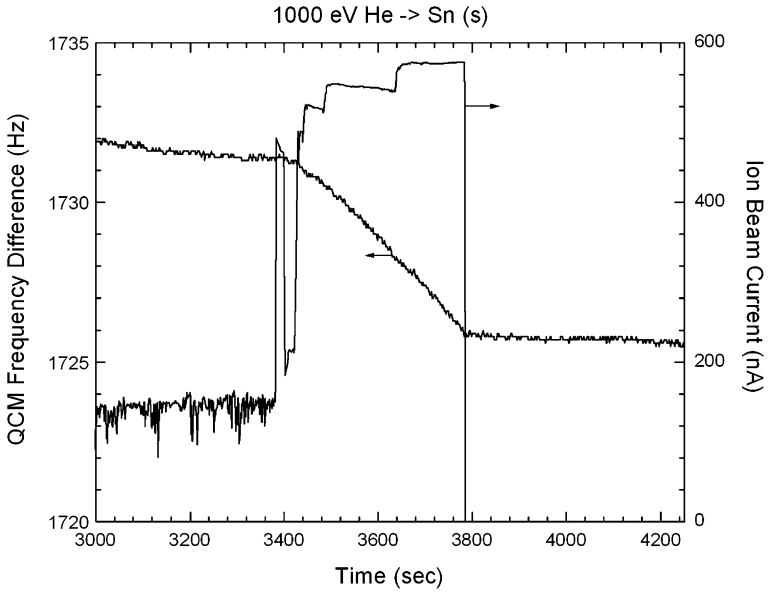

Fig. 2. Example of raw data recorded using IIAX. The change in crystal frequency is directly proportional to the mass deposited on it. Notice the three slopes shown, one with ~120 nA of ion current while the beam was being developed and focused onto the target, one with ~520 nA on target, and the last with the beam off. Even with the beam off there is a slightly negative slope due to oxidation on the crystal and evaporative flux, despite tin's low vapor pressure.

The other is a reference crystal, which is located to receive orders of magnitude less material than the deposition crystal, to monitor background effects on the crystal oscillation. The oscillators are in thermal contact and their frequency variation with time is closely recorded. The crystal and target planes are parallel, separated by 6 mm and with 6 mm of lateral separation of the centers of the target and the deposition crystal; the reference crystal is located 30 mm directly above the deposition crystal. This leads to 13% and 0.06% geometric collection efficiencies for the deposition and reference crystals, respectively. The quantity of interest is the temporal behavior of the difference of the two crystals' frequencies. The amount of mass deposited can be clearly discerned by analyzing the raw frequency difference plot versus time (see Fig. 2). This technique, along with its data interpretation, has been previously discussed in the context of IIAX [14–16].

3. Data analysis

Data analysis entailed measurement of the net amount of mass deposited upon the QCO surface from sputtering and the ion beam current (following adjustment for ion-induced electron and ion emission), consideration of the physical parameters and simultaneous processes, and finally, determination of the absolute sputtering yield. Provided that the mass of the deposited material is known, the total number of the sputtered particles can be obtained. For this particular case, it was assumed that tin oxide is formed on the surface of the QCO during bombardment due to similar fluxes of sputtered tin and molecular oxygen (based on 10^{-7} Pa O_2 partial pressure). Ex situ Auger emission spectroscopy (AES) analysis of the deposition crystal showed comparable levels of Sn and O in the layer under the adsorbed C and O layer on the surface justifying our assumption.

The first experimental parameter considered is the fraction of material ejected from the sample surface that strikes the crystal surface and adheres. This parameter is determined using two terms: one to account for the fraction of the sputtered material that strikes the surface (system geometry dependent), and one to quantify the amount of sputtered material that reflects from the surface (system chemistry dependent). The former is determined by assuming a cosine distribution of the sputtered material and taking into account the system geometry, and is typically near 13% for the IIAX system. The latter is estimated from experimental data of Fontell and Arminen [17] for Sn-on-Sn sticking coefficients. Based on average sputtered energy distributions calculated with VFTRIM [18], a variant of TRIM.SP [19], sticking coefficients of 50–60% were used.

A process that occurs simultaneously with deposition is the removal of deposited material from the crystal due

to bombardment by reflected particles from the ion beam. The strength of this effect is heavily dependent upon the beam species and energy in addition to the sample material. Geometric dependencies also play a role in this process as only a fraction of the reflected particles become incident upon the crystal face; the reflected-particle angular distribution is also approximated by using a cosine distribution for the reflected particles. VFTRIM estimated particle reflection (of incident ions) and sputtering (of reflected particles) coefficients and the mean sputtered (typically several eV) and reflected particle (near 60% of the initial) energies for these cases. The total uncertainty in the absolute sputtering yields due to experimental uncertainty and the use of the mentioned approximations can approach 40%.

4. Results and discussion

The experimental results of this investigation revealed that the liquid-tin sputtering yield due to He^+ and D^+ bombardment clearly depends upon surface temperature. From room temperature to 380 °C the sputtering yield due to irradiation by either species increased by factors of four to five, depending on the ion species and energy. As opposed to liquid lithium, liquid tin evaporation is negligible for these temperatures, and thus no correction for thermodynamic effects is necessary. Any enhancement measured in these experiments must be due to effects from ion-bombardment. Moreover, bubble-formation issues are excluded since the fluxes in these experiments were not greater than about 10^{18} $m^{-2}s^{-1}$. Figs. 3 and 4 display the data determined for helium- and deuterium-ion irradiation, respectively. The yield error bars combine experimental uncertainties and uncertainties inherent in our model; the temperature uncertainty is due to the measuring the temperature of a nearby surface and calibrating to the actual surface temperature instead of measuring it directly for this series of experiments. Note that a few of the solid points differ from those previously reported [7] due to the slightly oxidized nature of the earlier experiments. VFTRIM simulations were performed using an atomically smooth surface to enable comparison of standard sputtering models to our temperature-dependent data. The simulation results compared well with the room-temperature solid data.

We are confident in the clean nature of the surface of this most recent sample, as it was melted and remained molten for several hours, followed by resolidification prior to the experiments. This preparation process was based on the finding by Bastasz and Whaley [11,12] that surfaces of both liquid tin and solid tin that were previously melted in vacuo are oxygen-free within the temperature range considered. This condition is critical as tin is

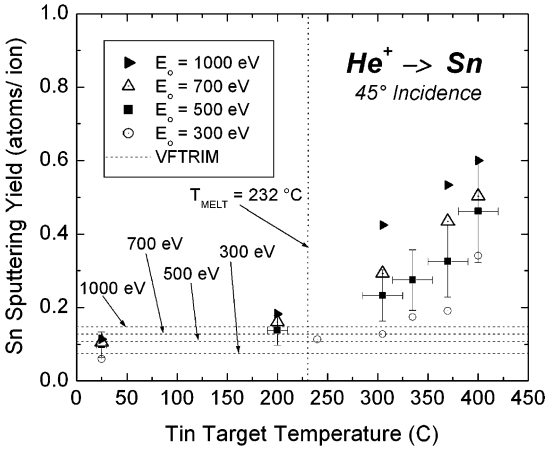

Fig. 3. Experimental results for the sputtering yield of liquid tin compared to solid due to helium ion bombardment; data are parameterized by the ion energy and presented as a function of target temperature. Representative error bars are shown for the 500 eV case – errors at the other energies are of similar magnitudes. VFTRIM results monotonically increase with ion energy for this particular energy range and have statistical uncertainty less than ±0.001 particles/ion.

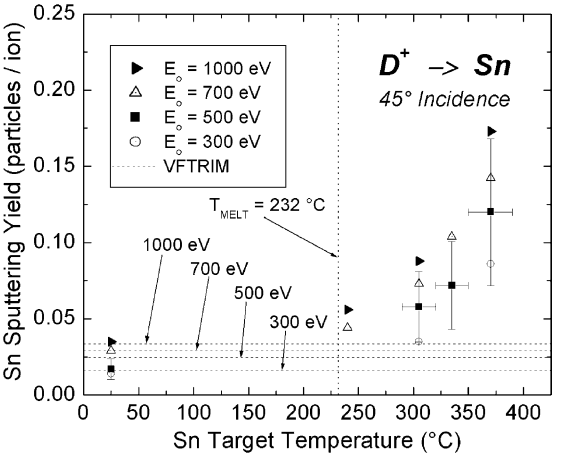

Fig. 4. Sputtering yield of liquid tin due to deuterium ion bombardment as a function of temperature. Error bars are only shown for the 500 eV case to reduce clutter; remaining error bars are comparable. Again, VFTRIM simulations showed monotonic increase of the sputtering yield over this range of ion energies and have statistical uncertainty less than $\pm 10^{-6}$ particles/ion.

one of only a few metals whose oxides have a higher sputtering yield than the pure metal in the solid state [13], as can be revalidated by comparing results from our previous study of the solid tin surface [7] with those shown here.

The level of temperature enhancement of liquid tin's sputtering yield from low-energy, light-ion bombard-

ment is similar to that of liquid gallium. The temperature dependence is clearly not as strong as that found in liquid lithium using similar ion species and energies in IIAX [4,5] or using a deuterium plasma with a target bias of 100 eV at PISCES-B [5] – where the sputtering yield increased by one to two orders of magnitude over a similar temperature range. Nonetheless, the temperature enhancement of liquid tin will play a key role in determining a realistic maximum operating temperature for a liquid tin divertor. This determination will also depend on the scrape-off-layer plasma parameters and the electronic properties of tin. Further iterative simulations using Monte Carlo codes such as REDEP [20–22], WBC [23,24], BBQ, LIM, DIVIMP, or ERO [1] should be performed with edge-plasma modeling programs, similar to those performed for the temperature-independent case [1], to more accurately determine this temperature limit as part of a thorough design of a liquid tin divertor.

The absolute sputtering yield of tin in the liquid state at 380 °C is about 0.4 particles/ion for 700 eV He^+ at 45°. Under similar bombardment conditions the yield for liquid Li is about 0.8 particles/ion. However, the ion-induced secondary ion fraction for lithium is high, 0.66 (where for most metals, including tin, the fraction is closer to 0.05). Therefore, in a fusion device with a magnetic sheath, only 1/3 of lithium sputtered particles will contribute to the impurity influx to the plasma. This results in a net *neutral* lithium-sputtering yield of about 0.27 Li atoms/ion. This could be a negative factor for the use of tin as plasma-facing components in a fusion device. In addition, the sputtering yields measured in IIAX are for low incident-ion fluxes ($\sim 10^{17}$–10^{18} $m^{-2}s^{-1}$). In the limit of high incident-ion flux, bubble formation is possible. Recent studies have found that bubble formation from He implantation in liquid Li is unclear or unlikely [25,26]. However, He bubbles are stable in liquid Sn due to its relatively high, almost 40% greater at their respective melting points [27], surface tension and could therefore be an additional erosion enhancement mechanism not measured in the present study. Further work with high incident-ion fluxes of the order of 10^{19}–10^{21} $m^{-2}s^{-1}$ is thus necessary to determine this effect and its implications for use of liquid Sn under realistic fusion device conditions, where incident fluxes are 10^{21}–10^{22} $m^{-2}s^{-1}$ or more.

The physical explanation of the temperature enhancement measured in IIAX and PISCES-B is incomplete. Two differing models have been proposed for the temperature enhancement of sputtering measured for liquid lithium. The Allain–Ruzic model, based on molecular dynamics simulations, claims the temperature dependence is due to the bonding nature of atoms near the surface with their nearest neighbor and the spatial distribution of deposited energy in a hot liquid as opposed to a solid [28]. The multi-body attractive forces at the surface are weakened with increasing temperature beyond the increase in thermal energy alone. The model asserts that incident particles deposit an increasing fraction of their energy in the near surface region as the temperature is increased. Molecular dynamic simulations need to be performed on the tin system to verify that these mechanisms are present in liquid tin in addition to liquid lithium. The effects of weakly-bound surface atoms at this interface and its role on the temperature dependence of liquid-metal erosion are still unclear and need further investigation.

An alternative model proposed by Doerner et al. [29] is the radiation-activated adatom sublimation model, or RAAS. In some ways similar to radiation-enhanced sublimation, RAAS claims that adatoms, particles with reduced bulk and surface binding energies, are created by energetic particle bombardment. With increasing temperature, the diffusion of adatoms to the surface increases and since adatoms are easier to evaporate, erosion is enhanced. However, the identity of 'adatoms' on the surface of liquid materials itself is not clear, and for a surface at thermodynamic equilibrium where T/T_m is close to unity, adatom and vacancy islands recombine and lower the overall adatom surface density [30].

For fusion application design, the temperature enhancement seen here is not much different from that reported for other liquid metals (e.g., Li, SnLi, Ga). Therefore, any liquid metal (and possibly molten salt) used in a magnetic fusion energy device (or any application involving plasma–liquid material interactions that has a finite tolerance for erosion and/or impurities) will, in part, determine the upper temperature limit via its temperature-enhanced sputtering yield; one exception to this is for high vapor pressure materials such as lithium, whose upper operating temperature can be limited by evaporative flux. In addition, further work is necessary to determine whether the magnitude of the incident ion flux also places a stronger restriction on the use of a particular liquid metal with respect to bubble stability, formation, and eruption, all of which can have strong temperature dependence.

5. Conclusions

Liquid Sn shows clear temperature enhancement of its sputtering yield under irradiation by low-energy light ions. The enhancement of the absolute sputtering yield increased with temperature by a factor ranging from two to six from ambient temperature to 420 °C. This measured temperature enhancement is on the order of that seen in liquid gallium [6], and not as severe as seen in liquid lithium [4,5]. This temperature enhancement, however, may not be inherent to all liquid materials, or all metals. It may show strong dependence upon the heat of sublimation and may even play a role in solid

materials. For example, the heats of sublimation of liquid metals that have shown an erosion enhancement with temperature are all relatively low (e.g., from 1.7 eV/atom for Li to 3.12 for Sn). The implications on fusion machine design have yet to be quantified, but there is strong evidence that temperature dependence of sputtering needs to be accounted for in future modeling. In addition, the role of bubble formation and its flux and temperature dependence need further investigation. Despite the imposition of this temperature limit and probable bubble-formation issues, liquid tin remains a promising candidate due to its comparatively low vapor pressure and weak retention of tritium.

Acknowledgments

The authors would like to thank Dan Rokusek and Donna Carpenter for their experimental and data analysis efforts, Ning Li for performing the AES analysis, Bob Bastasz for insightful discussions about the liquid tin surface, and Brian Jurczyk for helpful discussions regarding EUV light source technology. Funding for this project was provided by the Department of Energy contract DOE DEFG 0299ER54515. The AES was performed at the Center for the Microanalysis of Materials, University of Illinois, which is partially supported by the US Department of Energy under grant DEFG02-91-ER45439.

References

[1] J.N. Brooks, Fus. Eng. Des. 60 (2002) 515.
[2] M.A. Abdou, A. Ying, et al., On the Exploration of Innovative Concepts for Fusion Chamber Technology, Report: UCLA-ENG-99-206, UCLA, 1999.
[3] S. Sharafat, N. Ghoniem, Summary of Thermo-Physical Properties of Sn, and Compounds of Sn–H, Sn–O, Sn–C, Sn–Li, and Sn–Si and Comparison of Properties of Sn, Sn–Li, and Pb–Li, Report: UCLA-UCMEP-00-31, University of California, Los Angeles, 2000.
[4] J.P. Allain, M.D. Coventry, D.N. Ruzic, J. Nucl. Mater. 313–316 (2003) 641.
[5] R.P. Doerner, M.J. Baldwin et al., J. Nucl. Mater. 290–293 (2001) 166.
[6] R.W. Conn, R.P. Doerner et al., Nucl. Fusion 42 (2002) 1060.
[7] M.D. Coventry, J.P. Allain, D.N. Ruzic, J. Nucl. Mater. 313–316 (2003) 636.
[8] I.W. Choi, H. Daido et al., J. Opt. Soc. Am. B 17 (2000) 1616.
[9] J.P. Allain, PhD thesis, University of Illinois at Urbana-Champaign, 2001.
[10] J.P. Allain, Unpublished data, 2001.
[11] R. Bastasz, J. Whaley, Analysis of liquid tin surfaces, in: APEX/ALPS Meeting, PPPL, 2002.
[12] R. Bastasz, Personal Communication, 2002.
[13] R. Kelly, N.Q. Lam, Radiat. Eff. 19 (1973) 39.
[14] J.P. Allain, D.N. Ruzic, M.R. Hendricks, J. Nucl. Mater. 290–293 (2001) 33.
[15] J.P. Allain, D.N. Ruzic, M.R. Hendricks, J. Nucl. Mater. 290–293 (2001) 180.
[16] J.P. Allain, D.N. Ruzic, Nucl. Fusion 42 (2002) 202.
[17] A. Fontell, E. Arminen, Can. J. Phys. 47 (1969) 2405.
[18] D.N. Ruzic, Nucl. Instrum. and Meth. B 47 (1990) 118.
[19] J.P. Biersack, L.G. Haggmark, Nucl. Instrum. and Meth. 174 (1980) 257.
[20] J.N. Brooks, R.F. Mattas, A.M. Hassanein, J. Nucl. Mater. 128&129 (1984) 400.
[21] J.N. Brooks, Nucl. Tech./Fusion 4 (1983) 33.
[22] J.N. Brooks, J. Nucl. Mater. 111&112 (1982) 457.
[23] P.C. Stangeby, J.D. Elder, J. Nucl. Mater. 196–198 (1992) 258.
[24] J.N. Brooks, Phys. Fluids B 2 (1990) 1858.
[25] Z. Insepov, Personal Communication, 2003.
[26] D. Cowgill, Personal Communication, 2003.
[27] M. Shimoji, Liquid Metals: An Introduction to the Physics and Chemistry of Metals in the Liquid State, London, 1977.
[28] J.P. Allain, D.N. Ruzic, et al., Nucl. Instrum. and Meth. B, submitted for publication.
[29] R.P. Doerner, S. Krasheninnikov, S. Luckhardt, Personal Communication, 2003.
[30] C. Busse, C. Engin et al., Surf. Sci. 488 (2001) 346.